

Phonon-drag magnetoquantum oscillations in graphene

S. S. Kubakaddi,^{*} Tutul Biswas,[†] and Tarun Kanti Ghosh[‡]

^{*} Department of Physics, K. L. E. Technological University, Hubballi-580 031, Karnataka, India

[†] Department of Physics, Vivekananda Mahavidyalaya, Burdwan-713 103, West Bengal, India

[‡] Department of Physics, Indian Institute of Technology-Kanpur, Kanpur-208 016, Uttar Pradesh, India

(Dated: September 19, 2018)

A theory of low-temperature phonon-drag magnetothermopower S_{xx}^g is presented in graphene in a quantizing magnetic field. S_{xx}^g is found to exhibit quantum oscillations as a function of magnetic field B and electron concentration n_e . Amplitude of the oscillations is found to increase (decrease) with increasing B (n_e). The behavior of S_{xx}^g is also investigated as a function of temperature. A large value of S_{xx}^g (\sim few hundreds of $\mu\text{V}/\text{K}$) is predicted. Numerical values of S_{xx}^g are compared with the measured magnetothermopower S_{xx} and the diffusion component S_{xx}^d from the modified Girvin-Jonson theory.

PACS numbers: 72.10.Di, 72.80.Vp, 72.15.Jf, 65.80Ck

I. INTRODUCTION

Graphene, a monolayer of carbon atoms arranged in a honeycomb lattice of hexagons, has a unique band structure. Its electronic states, at the points \mathbf{K} and \mathbf{K}' of the Brillouin zone, have a linear dispersion relation, described by the Dirac equation. It is an ambipolar material with zero effective mass of the carriers and zero energy gap. Its electrical transport properties have been studied extensively^{1,2}, since its discovery³⁻⁵, with host of intriguing phenomena due to its unusual band structure. In a quantizing magnetic field \mathbf{B} , graphene exhibits the integer quantum Hall effect (QHE)^{4,5}, with novel features different from those in conventional two-dimensional electron gas (2DEG), particularly at $n = 0$ Landau level (LL).

Thermopower \mathbf{S} , an electric field \mathbf{E} generated in a sample due to unit temperature gradient i.e. $\mathbf{S} = \mathbf{E}/(-\nabla T)$, has been another powerful tool for probing carrier transport. Application of magnetic field \mathbf{B} , in addition to a temperature gradient ∇T , provides valuable experimental tool to investigate magnetothermoelectric effects. In a 2DEG, in the xy plane, a temperature gradient $\nabla T \parallel x$ -axis and magnetic field $\mathbf{B} \parallel z$ -axis generates electric field \mathbf{E} , in the sample, with components $E_x = S_{xx}(-\nabla T)_x$ and $E_y = S_{yx}(-\nabla T)_x$, where the thermopower S_{xx} and the Nernst-Ettingshausen coefficient S_{yx} are the tensor components of \mathbf{S} . Quantization effects due to magnetic field are reflected in thermopower.

In conventional 2DEG of GaAs heterojunctions (HJs) and Si-MOSFETs, magnetothermopower is investigated in detail, experimentally and theoretically, in the quantum Hall regime⁶⁻⁹. Measured magnetothermopower tensor components S_{xx} and S_{yx} exhibited oscillations as a function of magnetic field, arising due to crossing of Landau level by the Fermi level due to either change in carrier concentration or magnetic field. There are two additive and independent contributions to thermopower \mathbf{S} . In a ∇T , diffusion component \mathbf{S}^d arises due to diffusion of carriers and the phonon drag component \mathbf{S}^g arises due to the non-equilibrium phonons transferring some of their

momentum to the electrons via electron-phonon (el-ph) scattering. The oscillatory behavior of diffusion component is explained by the theory of Jonson and Girvin¹⁰ and Oji¹¹. It is established that for about $0.1 < T < 10$ K, the S^g contribution dominates S in GaAs HJs⁶⁻⁸. S^g is important because it gives directly el-ph coupling and is independent of impurity scattering, unlike mobility.

The study of phonon-drag magnetothermopower S^g , in conventional 2DEG, began with pioneering experimental work of Fletcher et al¹² showing the quantum oscillations as a function of B . Its B and T dependence were explained by developing the theory of S^g ¹³⁻¹⁵, by modifying the Boltzmann theory of phonon-drag in bulk semiconductors^{16,17}, following the II-approach due to Herring¹⁸.

In graphene, the experimental and theoretical investigations of thermoelectric effects in zero and quantizing magnetic field are being intensively pursued¹⁹. In monolayer graphene, experimental data of S vs T , in zero magnetic field, in temperature regime 10-300 K show largely linear behavior suggesting that the mechanism for thermopower is diffusive²⁰. Thermopower measurements in quantum Hall regime are carried out as a function of magnetic field for different gate voltage (i.e. for different carrier concentration) and temperatures²⁰⁻²³. Magnetothermopower S_{xx} and Nernst-Ettingshausen coefficient S_{yx} have shown the oscillatory behavior as a function of magnetic field. The behavior of S_{xx} and S_{yx} are in agreement with the generalized Mott relation, extending the theory of Jonson and Girvin¹⁰ to graphene²⁰. The peak values of S_{xx} are predicted to be given by $S_{xx}^{\text{peak}} = (-k_B/e) \ln 2/n$, noting that Jonson-Girvin theory fails for Landau level $n = 0$. Similar observations are made in high mobility samples of graphene²³. Zero-field non-linear T dependence is attributed to the screening²⁴. Measured strong quantum oscillations as a function of B are understood by evolution of the density of states at the Fermi level and S_{xx} becoming zero when the Fermi level lies in the localized states, because of absence of diffusion²³. In all these measurements, it is observed that phonon-drag thermopower component is absent and no evidence of

phonon-drag magnetoquantum oscillations, even at low temperatures, attributing to the weak el-ph coupling. We believe that, equally important reason for the absence of phonon-drag component in these samples may be due to their small size (~ 300 nm). It is about 10^4 times smaller than the samples of GaAs HJs (\sim mm in which S_{xx} is large and about \sim mV/K)⁶. At low temperatures, the smaller dimension of the sample sets the limit for phonon mean free path Λ , in the boundary scattering regime, as $S^g \sim \Lambda$. We expect the phonon-drag to be significant in large samples (few μ m) for e.g. in the samples of Nika et al²⁵. Moreover, to know the significant contribution of phonon-drag contribution, more data of S is required at low temperature covering sub-Kelvin region in pure samples.

The theory²⁶ of zero magnetic field S^g has been developed in monolayer graphene, in the boundary scattering regime, as a function of temperature T (≤ 10 K) and electron concentration n_e for the phonon mean free path $\Lambda \sim 10\mu$ m (closer to the samples of Nika et al²⁵). At about 10 K, $S^g \sim 10 \mu$ V/K. This value is nearly same order of magnitude as that of predicted S^d with the peak values few tens of μ V/K, by the modified Jonson-Girvin formula. We have to note that, unlike S^g , the latter is independent of sample size.

It would be interesting to study the effects of magnetic field quantization on phonon-drag thermopower S_{xx}^g . In the present work, we theoretically investigate the phonon-drag magnetothermopower as a function of magnetic field B , electron concentration n_e , and temperature T . We explore the circumstances and possibilities of its significant contribution to the measured magnetothermopower, by tuning the parameters B , n_e , T , and Λ . For comparison, we also compute diffusion component S_{xx}^d . The qualitative comparison of our calculations is made with the experimental observations.

This paper is organized as follows. In Sec. II, we provide formalism of phonon-drag thermopower in presence of quantizing magnetic field. In Sec. III, we present our results and discussion. A summary of our work is provided in Sec. IV.

II. FORMALISM OF PHONON-DRAG MAGNETOTHERMOPOWER

In the following we proceed with the calculations by appropriately modifying the theory of Fromhold et al¹⁵ for the monolayer graphene. We consider an isotropic and homogeneous 2DEG of graphene in the xy -plane with the magnetic field $\mathbf{B} = (0, 0, B)$ along the z -direction. In presence of an electric field \mathbf{E} (along x -axis) electrons are assumed to be accelerated isothermally ($\nabla T = 0$). In the steady state, the non-equilibrium distribution of the electrons in state α is given by $f_\alpha = f_\alpha^0 + f_\alpha^1$, where $f_\alpha^0 = [\exp\{(E_\alpha^0 - \mu_F)/k_B T\} + 1]^{-1}$ is the thermal equilibrium distribution function in absence of the electric field for state α , μ_F is the chemical potential and f_α^1 is the first-

order perturbation due to electric field E . These non-equilibrium electrons transfer some of their momentum to the 2D phonons through the el-ph coupling. This causes perturbation in the phonon distribution which is given by $N_{\mathbf{q}} = N_{\mathbf{q}}^0 + N_{\mathbf{q}}^1$, where $N_{\mathbf{q}}^0 = [\exp(\hbar\omega_{\mathbf{q}}/k_B T) - 1]^{-1}$ is the equilibrium distribution of the phonons of energy $\hbar\omega_{\mathbf{q}}$ and the wave vector \mathbf{q} . Here, $N_{\mathbf{q}}^1$ is the perturbation in the phonon distribution, due to electric field, producing the heat current density \mathbf{U} .

We confine our attention to the linear transport regime at liquid helium temperature. Then it is necessary to consider only acoustic phonons, with the 2D character, which interact weakly with the 2D electrons. The phonon heat current density, noting that $N_{\mathbf{q}}^0$ will not contribute, is given by

$$\mathbf{U} = A_0^{-1} \sum_{\mathbf{q}} N_{\mathbf{q}}^1 \hbar\omega_{\mathbf{q}} v_{\mathbf{q}}, \quad (1)$$

where $A_0 = L_x L_y$ is the area of graphene sample and $v_{\mathbf{q}}$ is the phonon group velocity.

In the linear response regime ($N_{\mathbf{q}}^1 \propto E$), the heat current density is given by $\mathbf{U} = \mathbf{M}\mathbf{E} = \mathbf{\Pi}\mathbf{J}$, where \mathbf{M} is the thermoelectric tensor, $\mathbf{\Pi} = \mathbf{M}/\boldsymbol{\sigma}$ is the Peltier coefficient tensor and $\boldsymbol{\sigma}$ is the electrical conductivity tensor. From the Onsager relation, the thermopower tensor is defined as $\mathbf{S} = \mathbf{\Pi}/T$. Using the Onsager symmetry relations it has been shown that¹⁵ $T S_{xx} = \rho_{xx} M_{xx} - \rho_{yx} M_{yx}$ and $T S_{yx} = \rho_{yx} M_{xx} + \rho_{xx} M_{yx}$, where S_{xx} and S_{yx} are, respectively, thermopower and Nernst-Ettingshausen coefficient, M_{xx} and M_{yx} are the components of tensor \mathbf{M} and ρ_{xx} and ρ_{yx} are the components of electrical resistivity tensor $\boldsymbol{\rho}$. Hence, the calculation of \mathbf{U} will facilitate the calculation of \mathbf{M} and hence S_{xx} and S_{yx} .

The solution for $N_{\mathbf{q}}^1$, in the linear response regime, is found to be

$$N_{\mathbf{q}}^1 = \frac{g}{k_B T} \sum_{\alpha, \alpha'} \tau_q \Gamma_{\alpha, \alpha'}(\mathbf{q}) \left[\frac{f_\alpha^1}{(\partial f_\alpha^0 / \partial E_\alpha)} - \frac{f_{\alpha'}^1}{(\partial f_{\alpha'}^0 / \partial E_{\alpha'})} \right], \quad (2)$$

where $g = g_s g_v$, $g_s(g_v)$ is the spin (valley) degeneracy, and

$$\Gamma_{\alpha, \alpha'}(\mathbf{q}) = P_{\alpha, \alpha'}^{\text{ab}0}(\mathbf{q}) f_\alpha^0 (1 - f_{\alpha'}^0), \quad (3)$$

$$P_{\alpha, \alpha'}^{\text{ab}0}(\mathbf{q}) = \frac{2\pi}{\hbar} |C_{\alpha, \alpha'}(\mathbf{q})|^2 N_{\mathbf{q}}^0 \delta(E_{\alpha'} - E_\alpha - \hbar\omega_{\mathbf{q}}). \quad (4)$$

Here, $P_{\alpha, \alpha'}^{\text{ab}0}(\mathbf{q})$ is the transition probability, in equilibrium, for the electron scattering from state α to state α' by absorbing a phonon and $|C_{\alpha, \alpha'}(\mathbf{q})|^2$ is the square of the electron-acoustic phonon interaction matrix element. Equation (2) is the general to the extent that, it is independent of the electronic structure and the type of el-ph coupling.

In a quantizing magnetic field $\mathbf{B} = (0, 0, B)$ with the Landau gauge $\mathbf{A} = (0, Bx, 0)$, the eigenfunctions and energy eigen values are given in Ref. [27]. The energy eigen values are $E_\alpha^0 = E_{n, k_y}^0 = \hbar\omega_c \sqrt{2n}$, where $\alpha \equiv (n, k_y)$, $n = 0, 1, 2, \dots$ is the Landau level quantum

number, k_y is the electron wave vector in the y -direction, $\omega_c = v_F/l_0$ is the cyclotron frequency, $v_F = 1 \times 10^6$ m/s is the Fermi velocity of electron in graphene, and $l_0 = \sqrt{\hbar/(eB)}$ is the magnetic length. The el-ph matrix element is given by (see Appendix A for details)

$$|C_{\alpha,\alpha'}(\mathbf{q})|^2 = |C(\mathbf{q})|^2 |J_{n,n'}(u)|^2 \delta_{k'_y, k_y + q_y}, \quad (5)$$

where $|C(\mathbf{q})|^2$ is the matrix which describes the el-ph coupling strength and $|J_{n,n'}(u)|$ with $u = q^2 l_0^2/2$, is the matrix element describing the scattering between Landau levels.

In presence of crossed electric field $\mathbf{E} = (E, 0, 0)$ and magnetic field $\mathbf{B} = (0, 0, B)$, the energy spectrum of graphene can be found exactly^{28,29}. In the linear response regime, where the applied electric field is low enough, one can obtain energy eigen value for the magnetic state α , approximately, as $E_\alpha \simeq E_\alpha^0 + eEx_\alpha$ by expanding the exact expression given in Refs. [28,29] up to first-order in $E/(v_F B)$. Here, $x_\alpha = k_y l_0^2$. This is nothing but the first-order energy correction due to the weak external electric field. Further, assuming that the form of distribution function retains the same with the modified energy, we expand $f_\alpha = f_0(E_\alpha) = f_0(E_\alpha^0) - eEx_\alpha [\partial f(E_\alpha^0)/\partial E_\alpha^0] (= f_0(E_\alpha^0) + f_\alpha^1)$, which gives $f_\alpha^1/[\partial f(E_\alpha^0)/\partial E_\alpha^0] = -eEx_\alpha$. Then, Eq. (2), using the momentum conservation $k'_y = k_y + q_y$, for the chosen Landau gauge gives,

$$N_q^1 = \frac{geEl_0^2}{k_B T} \sum_{\alpha\alpha'} \tau_q \Gamma_{\alpha\alpha'}(\mathbf{q}) q_y. \quad (6)$$

In order to make N_q^1 linear in E , we set all terms in $\Gamma_{\alpha\alpha'}(q)$ independent of E . Inserting Eq. (6) into Eq. (1) we write $\mathbf{U} = \mathbf{M}\mathbf{E}$ and take the phonon group velocity components $v_q^x = (q_x/q)v_s$ and $v_q^y = (q_y/q)v_s$, v_s being the acoustic phonon velocity in graphene. Then, the two components of the thermoelectric tensor \mathbf{M} are given by

$$M_{xx} = \frac{ge l_0^2 v_s}{A_0 k_B T} \sum_{\mathbf{q}} \tau_q \Gamma(\mathbf{q}) (q_x q_y / q) \hbar \omega_{\mathbf{q}} \quad (7)$$

$$M_{yx} = \frac{ge l_0^2 v_s}{A_0 k_B T} \sum_{\mathbf{q}} \tau_q \Gamma(\mathbf{q}) (q_y^2 / q) \hbar \omega_{\mathbf{q}}, \quad (8)$$

where

$$\Gamma(\mathbf{q}) = \sum_{\alpha\alpha'} \Gamma_{\alpha\alpha'}(\mathbf{q}). \quad (9)$$

When we carry out the angular integration, it can be seen that $M_{xx} = 0$ because of the xy isotropy. However, this is shown as the limitation of this theory as the experimental results of M_{xx} in conventional 2DEG show its non-zero value¹⁵. Later calculations in these systems, taking into account of anisotropy of electrons and phonons, remove this limitation³⁰. However, in the present work we undertake the evaluation of only M_{yx} , as we have considered xy isotropy of the system.

Using Eqs. (3) and (4), Eq. (9) turns out to be

$$\Gamma(\mathbf{q}) = \frac{2\pi}{\hbar} \sum_{\alpha} \sum_{\alpha'} |C_{\alpha,\alpha'}(\mathbf{q})|^2 N_{\mathbf{q}}^0 f^0(E_{\alpha}^0) \times [1 - f^0(E_{\alpha'}^0)] \delta(E_{\alpha'}^0 - E_{\alpha}^0 - \hbar\omega_{\mathbf{q}}). \quad (10)$$

Summation of over k'_y is carried out replacing it by $k_y + q_y$. Since the integrand is independent of k_y , summation over k_y simply gives $A_0/2\pi l_0^2$.

In the presence of disorder, the energy levels (in zero electric field) E_{n,k_y}^0 and $E_{n,k_y+q_y}^0$ are randomized by LL broadening. A simple system average is taken by integrating over $\epsilon = E_{n,k_y}^0$ and $\epsilon' = E_{n,k_y+q_y}^0$ with the weight factor $\rho(\epsilon - E_n^0)\rho(\epsilon' - E_{n'}^0)$, where $E_n^0(E_{n'}^0)$ is the energy of the $n(n')$ -th LL in absence of disorder and $\rho(x)$ is the LL density of states with convenient line shape function. Now Eq. (10) becomes

$$\Gamma(\mathbf{q}) = \frac{A_0}{2\pi l_0^2} \frac{2\pi}{\hbar} \sum_n \sum_{n'} |C_{n,n'}(\mathbf{q})|^2 N_{\mathbf{q}}^0 \times \int d\epsilon d\epsilon' f^0(\epsilon) [1 - f^0(\epsilon')] \delta(\epsilon' - \epsilon - \hbar\omega_{\mathbf{q}}) \rho(\epsilon - E_n^0) \rho(\epsilon' - E_{n'}^0). \quad (11)$$

Integration with respect to ϵ' , using the Dirac delta function, gives

$$\Gamma(\mathbf{q}) = \frac{A_0}{\hbar l_0^2} \sum_n \sum_{n'} |C(\mathbf{q})|^2 |J_{n,n'}(u)|^2 N_{\mathbf{q}}^0 I_{nn'}(\hbar\omega_{\mathbf{q}}), \quad (12)$$

where

$$I_{nn'}(\hbar\omega_{\mathbf{q}}) = \int d\epsilon f^0(\epsilon) [1 - f^0(\epsilon + \hbar\omega_{\mathbf{q}})] \rho(\epsilon - E_n^0) \rho(\epsilon + \hbar\omega_{\mathbf{q}} - E_{n'}^0). \quad (13)$$

Since the phonon-drag thermopower is important at low temperature, the energy of acoustic phonons involved is so small that only intra LL scattering is possible. Thus we set $n = n'$ in Eq. (12). Then, with

$$|J_{nn}(u)|^2 = \frac{e^{-u}}{4} \left[L_n(u) + L_{n-1}(u) \right]^2, \quad (14)$$

Equation (12) gives

$$\Gamma(\mathbf{q}) = \frac{A_0}{\hbar l_0^2} |C(\mathbf{q})|^2 N_{\mathbf{q}}^0 \sum_n |J_{nn}(u)|^2 I_{nn}(\hbar\omega_{\mathbf{q}}). \quad (15)$$

Intra LL transitions are possible as the energy levels are broadened.

Using Eq. (15) in Eq. (8), we get

$$M_{yx} = \frac{ge v_s}{\hbar k_B T} \sum_{\mathbf{q}} \tau_q (q_y^2 / q) \hbar \omega_{\mathbf{q}} |C(\mathbf{q})|^2 N_{\mathbf{q}}^0 \times \sum_n |J_{nn}(u)|^2 I_{nn}(\hbar\omega_{\mathbf{q}}). \quad (16)$$

The summation over \mathbf{q} is converted into integration as

$$\sum_{\mathbf{q}} \rightarrow \frac{A_0}{(2\pi)^2} \int_0^\infty q dq \int_0^{2\pi} d\theta. \quad (17)$$

Angular integration coming through $q_y = q \sin \theta$ gives π . Then

$$M_{yx} = \frac{geA_0}{4\pi\hbar^4 v_s^2 k_B T} \int_0^\infty d(\hbar\omega_q) \tau_q (\hbar\omega_q)^3 |C(q)|^2 N_q^0 \times \sum_n |J_{nn}(u)|^2 I_{nn}(\hbar\omega_q). \quad (18)$$

Substituting for $|C(q)|^2 = D^2 \hbar\omega_q / (2\rho_m A_0 v_s^2)$, where D is the acoustic phonon deformation potential coupling constant and ρ_m is the areal mass density of graphene, we obtain

$$M_{yx} = \frac{geD^2}{8\pi\rho_m \hbar^4 v_s^4 k_B T} \int_0^\infty d(\hbar\omega_q) \tau_q (\hbar\omega_q)^4 N_q^0 \times \sum_n |J_{nn}(u)|^2 I_{nn}(\hbar\omega_q). \quad (19)$$

From Onsager relation, with $M_{xx} = 0$, we have $T S_{xx}^g = -\rho_{yx} M_{yx}$. Taking $\rho_{yx} = B / (n_e e)$ ³¹, where n_e is the electron density and expressing B in terms of l_0^2 , we get

$$S_{xx}^g = -\frac{gk_B D^2}{8\pi e \rho_m \hbar^3 v_s^4 l_0^2 n_e (k_B T)^2} \int_0^\infty d(\hbar\omega_q) \tau_q (\hbar\omega_q)^4 N_q^0 \times \sum_n |J_{nn}(u)|^2 I_{nn}(\hbar\omega_q). \quad (20)$$

We note that this equation can also be obtained by following the method of Kubakaddi et al¹³ for conventional 2DEG ignoring $\Gamma(q)$ compared to $1/\tau_q$.

III. RESULTS AND DISCUSSION

Since $S_{xx}^g \sim \Lambda$ and D^2 , it is essential to choose the reasonable values of these parameters. We numerically evaluate S_{xx}^g , for $T \leq 20$ K in the boundary scattering regime for which $\tau_q = \Lambda / v_s$, where Λ is the phonon mean free path. Normally, Λ is taken to be the smaller dimension of the sample. Thermal conductivity calculations are demonstrated with Λ chosen in the range of 3-30 μm and the choice of $\Lambda = 5$ μm is giving reasonable agreement with the measured thermal conductivity^{25,32}. Nika et al²⁵, to fit the thermal conductivity data, use the effective phonon mean free path $\Lambda_{\text{eff}} = \Lambda(1+p)/(1-p)$ by modulating the smallest dimension of the sample using specular parameter $p = 0.9$, which enhances Λ by a factor of 20. The value of $0 \leq p \leq 1$ is determined by the roughness of the graphene edges. To present our calculations we choose a reasonable value of $\Lambda = 10$ μm .

In the literature there is a range of $D = 3\text{-}30$ eV. We chose $D = 20$ eV which is closer to the values of D , for unscreened el-phon interaction, used to fit the experimental

data of some of the transport properties³³⁻³⁶. The line shape function $\rho(x)$ of LL is taken to be Lorentzian with the width $\Gamma = C\sqrt{B}$, where $C = 0.5$ meV/ $\sqrt{\text{Tesla}}$. Other parameter values used are: $\rho_m = 7.6 \times 10^{-7}$ Kg/m² and $v_s = 2 \times 10^4$ m/s.

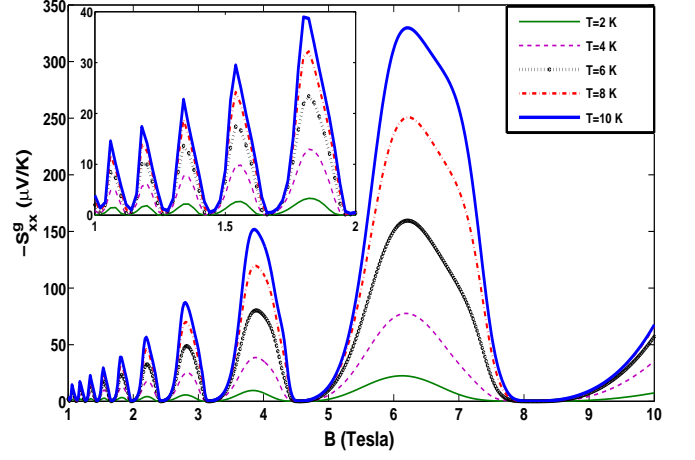


FIG. 1: (Color online) Plots of phonon-drag thermopower S_{xx}^g versus magnetic field B at five different temperatures, namely, $T = 2, 4, 6, 8,$ and 10 K for $n_e = 10^{16}$ m⁻² and $\Lambda = 10$ μm . Inset shows the behavior of S_{xx}^g in the low field regime.

In Fig. 1, S_{xx}^g is shown as a function of B , for $T = 2, 4, 6, 8, 10$ K for $n_e = 1 \times 10^{16}$ m⁻². We see that S_{xx}^g is oscillatory with the height of the peak increasing with the increasing B . The position of the peak occurs when the Fermi energy is in the localized state of LL. Interestingly, our calculations show large peak values of the order of few hundreds of $\mu\text{V/K}$ which is closer to the values observed in GaAs HJs^{12,37}. We would like to point out that the sample size in GaAs HJs (\sim few mm) is about two orders of magnitude larger than the size of the graphene sample chosen here. The size of the graphene sample (300 nm) in the experiment of Zuev et al²⁰ is about 30 times smaller than the value of Λ used in the present calculation. Scaling the Λ down by 30 times, we get the peak values of S_{xx}^g few tens of $\mu\text{V/K}$ which is comparable to the measured values.

Dependence of S_{xx}^g on n_e is shown in Fig. 2 for three different magnetic fields, namely $B = 2.82, 3.88,$ and 6.20 Tesla, at $T = 5$ K taking $\Lambda = 10$ μm . Again, the behavior is found to be oscillatory. This is similar to the behavior observed (as function of gate voltage) in the experiment of Zuev et al²⁰. The peak value of S_{xx}^g is decreasing with the increasing n_e . This is similar to the n_e dependence of zero field S^g and S^d ²⁶. Also, it is found that the peak values are smaller for smaller B . The number of oscillations contained in S_{xx}^g gets reduced with the increase of magnetic field. This is due to the increase of the separation between LLs with increasing magnetic field. Interestingly, we note that the position of the peak values corresponding to three different B are coinciding

at $n_e = (1, 4, 7 \text{ and } 10) \times 10^{16} \text{ m}^{-2}$.

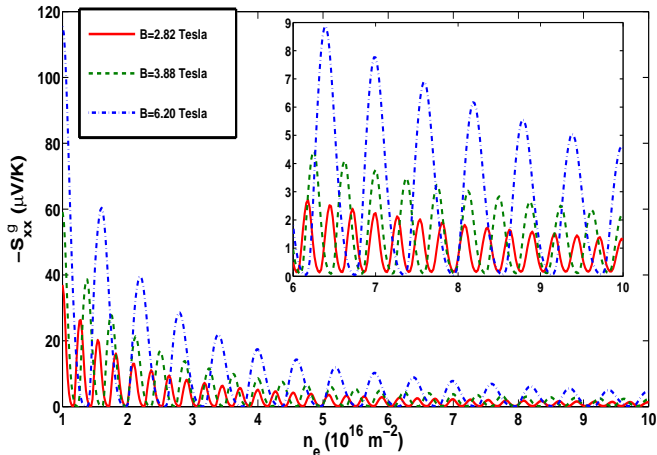


FIG. 2: (Color online) Plots of phonon-drag thermopower S_{xx}^g versus carrier density n_e at different magnetic fields, namely, $B = 2.82, 3.88,$ and 6.20 Tesla for $T = 5$ K and $\Lambda = 10$ μm . The behavior of S_{xx}^g around the higher density regime is depicted in the inset.

In Fig. 3(a), we have shown S_{xx}^g as a function of n_e for $\Lambda = 300$ nm (as taken in Ref. [20]) at temperatures $T = 4.2, 10,$ and 20 K for a magnetic field $B = 8.8$ Tesla. For comparison, we have calculated diffusion component S_{xx}^d as a function of n_e , for the same T and B , using modified Girvin-Jonson theory (see Ref. [21]) and it is shown in Fig. 3(b). Note that S_{xx}^d is also found to decrease with increasing n_e . According to the Girvin-Jonson theory, the peak values due to diffusion component are given by $(k_B/e)\ln 2/n$. S_{xx}^d is found to be much greater than S_{xx}^g . For example, for $n_e \sim 1.5 \times 10^{12} \text{ cm}^{-2}$, at 4.2 K (10 K) S_{xx}^d is nearly ten (three) times greater than S_{xx}^g . The total $S_{xx} = S_{xx}^d + S_{xx}^g$ is shown as a function of n_e in Fig. 3(c) and it is increasing with T .

We would like to point out that in graphene, the peak values of diffusion thermopower S_{xx}^d are quantized as $(k_B/e)\ln 2/n$ which differs from the peak value quantization $(k_B/e)\ln 2/(n + 1/2)$ corresponding to the conventional 2DEG. This difference is attributed to the existence of a non-trivial Berry phase π in graphene²¹. Unlike diffusion thermopower, it is difficult to establish such peak value quantization for S_{xx}^g . However, a careful observation of Fig. 3(a) & 3(b) dictates us that S_{xx}^g follow S_{xx}^d with respect to the locations of peaks. Moreover, the locations of thermopower peaks in 2DEG and graphene are expected to be different due to different Landau level structures as was found in the case of conductivity oscillations²⁷.

In Fig 4, we have shown S_{xx}^g as function of T for $B = 2.82, 3.88$ and 6.20 Tesla (corresponding to three peak values in Fig. 1). S_{xx}^g increases with increasing T , more rapidly at lower T . At higher T , the increase is slower and showing nearly independent behavior for about $T > 10$ K. This behavior is similar to the obser-

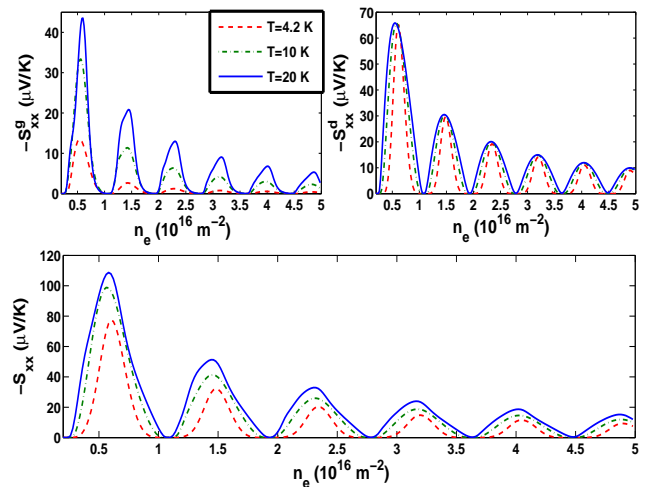


FIG. 3: (Color online) Plots of thermopower versus carrier density n_e at different temperature for $B = 8.8$ Tesla and $\Lambda = 300$ nm as considered in Ref.[20]. Here, (a) S_{xx}^g , (b) S_{xx}^d , (c) $S_{xx} = S_{xx}^g + S_{xx}^d$.

vations in conventional 2DEG^{12–14}. The faster increase of S_{xx}^g with T , at low T , may be attributed to the increasing number of phonons linearly with T . For a given magnetic field, maximum momentum transfer takes place when $\hbar v_s q \simeq \Gamma$ setting limit on q . As T increases further, the allowed q is limited by the width of LL ($\Gamma \sim B^{1/2}$) and fewer phonons will exchange momentum. In zero magnetic field, such behavior is generally interpreted^{6,8} in terms of the dominant phonon wave vector q_D and Fermi wave vector $2k_F$. At a given T , S_{xx}^g is larger for larger B . This is consistent with the findings in conventional 2DEG^{12,14}.

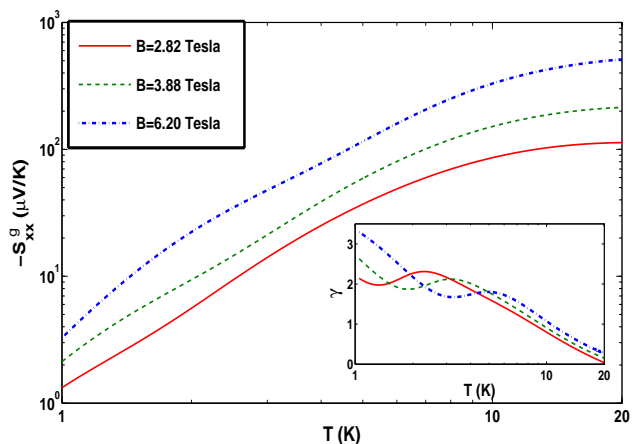


FIG. 4: (Color online) Temperature dependence of phonon-drag thermopower at electron density $n_e = 10^{16} \text{ m}^{-2}$. Inset shows variation of the exponent $\gamma = d \ln S_{xx}^g / d \ln T$ with temperature.

Inset of Fig. 4, expressing $S_{xx}^g \sim T^\gamma$, shows the behavior of exponent γ as a function of T for different B . It is found to decrease and tending to zero with increasing T . Moreover, γ is found to be larger for larger B . We observe that for T closer to 1 K, γ is greater than 2 which is signature of phonon-drag thermopower. When S_{xx}^g is calculated as a function of T (not shown in the figure) for different n_e we expect it to increase with increasing T but to be smaller for larger n_e . These curves are expected to show again nearly independent behavior at higher T , more so for smaller n_e . Exponent γ , in this case n_e dependent, is again expected to decrease with increasing T .

Important point we notice is that S_{xx}^g can be tailored to be as large as few mV/K by reducing n_e and working at larger B . We suggest that the enhanced phonon drag contribution S_{xx}^g can be achieved by polishing the edge of the sample. It is characterized by a specular parameter p with its value $0 < p < 1$. The perfect reflecting edge gives $p = 1$ and very rough edge corresponds to $p = 0$ (diffusive scattering). Besides, the larger samples can be grown on piezoelectric substrates. Woszczyna et al³⁸ have shown that the graphene samples as large as $150 \times 30 \mu\text{m}^2$ on GaAs substrate can be prepared.

We would like to point out that the screening of el-ph coupling in magnetic field is ignored, although justification is for zero magnetic field case. In conventional 2DEG screening is found to reduce the phonon drag thermopower significantly both in zero and quantizing magnetic field⁶⁻⁹. However, screening of el-ph interaction in graphene in magnetic field is yet to be established. Low temperature experimental S_{xx}^g may throw some light on significance of screening. One can extract the experimental phonon drag S_{xx}^g from the experimentally measured S_{xx} values by subtracting diffusion component using generalized Mott formula²⁰.

IV. SUMMARY

In summary, we have studied phonon-drag thermopower S_{xx}^g in graphene subjected to a transverse magnetic field. Based on a method, described in Ref.[15], a modified theory is developed to calculate S_{xx}^g quantitatively. Dependence of S_{xx}^g on magnetic field, electron density, and temperature have been studied. With both magnetic field and density, S_{xx}^g exhibits oscillatory behavior. Interestingly, we have found an enhanced phonon-drag thermopower with magnitude of the order of few hundreds $\mu\text{V}/\text{K}$. This value is closer to that obtained in the case of conventional 2DEG at GaAs based semiconductor hetero interface. We attribute this enhanced phonon-drag effect is a consequence of taking the high value of phonon-mean free path, namely, $\Lambda = 10 \mu\text{m}$. We, thus, suggest that phonon-drag effect may have significant contribution in larger samples of graphene. We have also shown the density dependence of S_{xx}^g for parameter values which were taken in Ref.[20]. The diffu-

sion thermopower has also been calculated for the sake of comparison using modified Girvin-Jonson theory. Moreover, the temperature dependence of S_{xx}^g is also studied and the exponent of this dependence has been extracted.

Acknowledgement

SSK would like to thank M. Tsaousidou and TKG would like to thank A. Kundu for useful discussions.

Appendix A

1. Matrix elements of Electron-phonon coupling in a magnetic field

For a graphene monolayer, lying in xy plane, with a perpendicular magnetic field $\mathbf{B} = (0, 0, B)$, the eigen functions, for Landau gauge $\mathbf{A} = (0, Bx, 0)$, are given by²⁷

$$\psi_\alpha(\mathbf{r}) = \frac{e^{ik_y y}}{\sqrt{L_y}} \chi_{n,k_y}(x) \quad (\text{A1})$$

with

$$\chi_{n,k_y}(x) = \frac{1}{\sqrt{2}} \begin{pmatrix} -i\phi_{n-1}(x) \\ \phi_n(x) \end{pmatrix}. \quad (\text{A2})$$

Here, $\alpha \equiv (n, k_y)$, $n = 0, 1, 2, 3, \dots$ is the Landau level index, k_y is the y -component of electron wave vector, $\phi_n(x) = \sqrt{1/(2^n n! \sqrt{\pi} l_0)} e^{-(x+x_0)^2/(2l_0^2)} H_n[(x+x_0)/l_0]$ with $x_0 = l_0^2 k_y$ is the harmonic oscillator wave function.

We assume that at low temperature, for the graphene on the substrate, electrons interact with only in-plane acoustic phonons via deformation potential coupling. In suspended graphene, there will be flexural modes, whose contribution is neglected for the graphene on substrate³⁹. The deformation potential coupling is assumed to be only due to longitudinal acoustic phonons.

The most general form of electron-phonon interaction Hamiltonian is

$$H_{ep}(\mathbf{r}) = \sum_{\mathbf{q}s} \left[V_{\mathbf{q}s} e^{i\mathbf{q}\cdot\mathbf{r}} a_{\mathbf{q}s} + V_{\mathbf{q}s}^\dagger e^{-i\mathbf{q}\cdot\mathbf{r}} a_{\mathbf{q}s}^\dagger \right],$$

where $a_{\mathbf{q}s}$ ($a_{\mathbf{q}s}^\dagger$) is the phonon annihilation (creation) operator and $V_{\mathbf{q}s}$ is the matrix element of a particular phonon mode (\mathbf{q}, s) . For longitudinal acoustic phonon mode corresponding to deformation potential, the form of $V_{\mathbf{q}s}$ is given by $V_q = D[\hbar\omega_q/(2A_0\rho_m v_s^2)]^{1/2}$, where A_0 is the area of graphene sample, D is the deformation potential coupling constant, and ρ_m is the areal mass density of graphene. The electron-acoustic phonon matrix element, for the scattering between the states $\alpha \equiv (n, k_y)$ and $\alpha' \equiv (n', k'_y)$, is given by

$$C_{\alpha,\alpha'}(q) = \int \psi_{\alpha'}^\dagger(\mathbf{r}) V_q e^{i\mathbf{q}\cdot\mathbf{r}} \psi_\alpha(\mathbf{r}) d^2r. \quad (\text{A3})$$

Substituting for $\psi_\alpha(\mathbf{r})$ and $V_{\mathbf{q}}$, we get Eq. (5) in which the integrals are given by

$$C_{k'_y, k_y} = \frac{V_q}{L_y} \int_0^{L_y} e^{-i(k'_y - k_y - q_y)y} dy = C(q) \delta_{k'_y, k_y + q_y} \quad (\text{A4})$$

and

$$J_{n, n'}(u) = \int_{-\infty}^{\infty} \chi_{n', k'_y}^\dagger(x) e^{iq_x x} \chi_{n, k_y}(x) dx. \quad (\text{A5})$$

At low temperature, the acoustic phonon energy is small and cause only intra-Landau level transitions ($n = n'$). Inter-Landau level transitions are expected at higher temperatures and in the studies such as magnetophonon

resonance in which optical phonons are involved⁴⁰. The matrix element corresponding to intra-Landau level transitions is found to be

$$C_{\alpha, \alpha'}(q) = C(q) J_{nn}(u) \delta_{k'_y, k_y + q_y} \quad (\text{A6})$$

where

$$J_{nn}(u) = \frac{1}{2} e^{iq_x x_0} e^{-\frac{u}{2}} \left[L_{n-1}(u) + L_n(u) \right] \quad (\text{A7})$$

with $u = q^2 l_0^2 / 2$. The equation for $|J_{nn}(u)|^2$ given in Eq.(14) is similar to the one obtained in Refs.[41,42].

-
- * Electronic address: sskubakaddi@gmail.com
† Electronic address: tbtutulum53@gmail.com
‡ Electronic address: tkghosh@iitk.ac.in
- ¹ A. H. Castro Neto, F. Guinea, N. M. R. Peres, K. S. Novoselov, and A. K. Geim, *Rev. Mod. Phys.* **81**, 109 (2009).
 - ² S. Das Sarma, S. Adam, E. H. Hwang, and E. Rossi, *Rev. Mod. Phys.* **83**, 407 (2011).
 - ³ K. S. Novoselov, A. K. Geim, S. V. Morozov, D. Jiang, Y. Zhang, S. V. Dubonos, I. V. Grigorieva, and A. A. Firsov, *Science* **306**, 666 (2004).
 - ⁴ K. S. Novoselov, A. K. Geim, S. V. Morozov, D. Jiang, M. I. Katsnelson, I. V. Grigorieva, S. V. Dubonos, and A. A. Firsov, *Nature (London)* **438**, 197 (2005).
 - ⁵ Y. Zhang, Y. W. Tan, H. L. Stormer, and P. Kim, *Nature (London)*, **438**, 201 (2005).
 - ⁶ B. L. Gallagher and P. N. Butcher, in *Handbook on Semiconductors*, Vol 1, Eds. P. T. Landsberg, (Elsevier, Amsterdam, 1992) p 817.
 - ⁷ R. Fletcher, *Semicond. Sci. Technol.* **14**, R1 (1999).
 - ⁸ R. Fletcher, E. Zaremba, and U. Zeitler, in *Electron-Phonon Interactions in Low-Dimensional Structures*, Ed L. Challis (Oxford: Oxford Science Publications, 2003) p 149.
 - ⁹ M. Tsousidou, *The Oxford Handbook of Nanoscience and Technology*, vol II, ed A. V. Narlikar and Y. Y. Yu (Oxford: Oxford University Press, 2010) p 477.
 - ¹⁰ M. Jonson and S. M. Girvin, *Phys. Rev. B* **29**, 1939 (1984).
 - ¹¹ H. Oji, *J. Phys. C* **17**, 3059 (1984).
 - ¹² R. Fletcher, J. C. Maan, K. Ploog, and G. Weimann, *Phys. Rev. B* **33**, 7122 (1986).
 - ¹³ S. S. Kubakaddi, P. N. Butcher, and B. G. Mulimani, *Phys. Rev. B* **40**, 1377 (1989).
 - ¹⁴ S. K. Lyo, *Phys. Rev. B* **40**, 6458 (1989).
 - ¹⁵ T. M. Fromhold, P. N. Butcher, G. Qin, B. G. Mulimani, J. P. Oxley, and B. L. Gallagher, *Phys. Rev. B* **48**, 5326 (1993).
 - ¹⁶ J. P. Jay-Gerin, *Phys. Rev. B* **12**, 1418 (1975).
 - ¹⁷ S. M. Puri, *Phys. Rev.* **139**, A995 (1965).
 - ¹⁸ C. Herring, *Phys. Rev.* **96**, 1163 (1954).
 - ¹⁹ N. S. Sankeshwar, S. S. Kubakaddi, and B. G. Mulimani, *Graphene Science Handbook: Electrical and Optical Properties*, Eds. M. Aliofkhaezrai, N. Ali, W. I. Milne, C. S. Ozkan, S. Mitura, J. L. Gervasoni, CRC Hand Book, CRC Press, (Taylor and Francisco group, New York, 2016) Vol. 18, pp. 273.
 - ²⁰ Y. M. Zuev, W. Chang, and P. Kim, *Phys. Rev. Lett.* **102**, 096807 (2009).
 - ²¹ J. G. Checkelsky and N. P. Ong, *Phys. Rev. B* **80**, 081413(R) (2009).
 - ²² P. Wei, W. Bao, Y. Pu, C. N. Lau, and J. Shi, *Phys. Rev. Lett.* **102**, 166808 (2009).
 - ²³ X. Wu, Y. Hu, M. Ruan, N. K. Madiomanana, C. Berger, and W. A. de Heer, *Appl. Phys. Lett.* **99**, 133102 (2011).
 - ²⁴ E. H. Hwang, E. Rossi, and S. Das Sarma, *Phys. Rev. B* **80**, 235415 (2009).
 - ²⁵ D. L. Nika, E. P. Pokatilov, A. S. Askerov, and A. A. Balandin, *Phys. Rev. B* **79**, 155413 (2009).
 - ²⁶ S. S. Kubakaddi, *Phys. Rev. B* **79**, 075417 (2009).
 - ²⁷ A. Matulis and F. M. Peeters, *Phys. Rev. B* **75**, 125429 (2007).
 - ²⁸ V. Lukose, R. Shankar, and G. Baskaran, *Phys. Rev. Lett.* **98**, 116802 (2007).
 - ²⁹ N. M. R. Peres and E. V. Castro, *J. Phys.: Condens. Matter* **19**, 406231 (2007).
 - ³⁰ P. N. Butcher and M. Tsousidou, *Phys. Rev. Lett.* **80**, 1718 (1998).
 - ³¹ R. P. Tiwari and D. Stroud, *Phys. Rev. B* **79**, 165408 (2009).
 - ³² S. Ghosh, D. L. Nika, E. P. Pokatilov, and A. A. Balandin, *New J. Phys.* **11**, 095012 (2009).
 - ³³ A. M. R. Baker, J. A. Alexander-Webber, T. Althebaeumer, S. D. McMullan, T. J. B. M. Janssen, A. Tzalenchuk, S. Lara-Avila, S. Kubatkin, R. Yakimova, C. T. Lin, L. J. Li, and R. J. Nicholas, *Phys. Rev. B* **87**, 045414 (2013).
 - ³⁴ J. Huang, J. A. Alexander-Webber, T. J. B. M. Janssen, A. Tzalenchuk, T. Yager, S. Lara-Avila, S. Kubatkin, R. L. Myers-Ward, V. D. Wheeler, D. K. Gaskill, and R. J. Nicholas, *J. Phys.: Condens. Matter* **27**, 164202 (2015).
 - ³⁵ R. Bistrizer and A. H. MacDonald, *Phys. Rev. B* **80**, 085109 (2009).
 - ³⁶ A. M. DaSilva, K. Zou, J. K. Jain, and J. Zhu, *Phys. Rev. Lett.* **104**, 236601 (2010).
 - ³⁷ B. Tieke, R. Fletcher, U. Zeitler, M. Henini, and J. C. Maan, *Phys. Rev. B* **58**, 2017 (1998).
 - ³⁸ M. Woszczyna, M. Friedemann, M. Götz, E. Pesel, K. Pierz, T. Weimann, and F. J. Ahlers, *Appl. Phys. Lett.* **100**, 164106 (2012).

- ³⁹ E. Mariani and F. von Oppen, Phys. Rev. B **82**, 195403 (2010)
- ⁴⁰ M. O. Goerbig, J. N. Fuchs, K. Kechedzhi, and V. I. Fal'ko, Phys. Rev. Lett. **99**, 087402 (2007).
- ⁴¹ K. Nomura and A. H. MacDonald, Phys. Rev. Lett. **96**, 256602 (2006).
- ⁴² B. S. Kandemir and A. Mogulkoc, Phys. Lett. A **379**, 2120 (2015).